Eur. Phys. J. C 46, s01, 37–43 (2006)
Digital Object Identifier (DOI) 10.1140/epjcd/s2006-02-003-9

EPJ C direct
electronic only

Scientific Note

Jet Calibration using γ+Jet Events in the CMS Detector

V. Konoplianikov[1], A. Ulyanov[2], O. Kodolova[3]

[1] JINR, Dubna, Russia, on leave from GSU, Gomel, Belarus
[2] ITEP, Moscow, Russia
[3] Moscow State University, Moscow, Russia

Received: 14 March 2006 / Revised version: 5 April 2006 /
Published online: 7 June 2006 –

Abstract. A procedure is presented for evaluating the jet energy scale from direct photons in γ+jet events. The systematic shifts obtained on the jet energy scale with this technique are estimated. The range of applicability of this channel to calibrate the data is also discussed. The study is conducted using fully simulated events passed through the CMS detector including the effects of pile-up at an instantaneous luminosity of $\mathcal{L} = 2 \times 10^{33}\,\mathrm{cm}^{-2}\mathrm{s}^{-1}$.

1 Introduction

This note describes a procedure for setting the jet energy scale using direct photons in the process γ+jet. Assuming negligible total transverse momentum in the initial state of the scattering process, the direct photon produced in γ+jet events has a transverse momentum that is equal and opposite to the recoiling jet. The high resolution ($\sim 1\%$) of the electromagnetic calorimeter provides an accurate measurement of the photons and through the direct kinematical relationship is the basis of the jet calibration procedure. Jet calibration using γ+jet events is successfully employed by D0 Collaboration who have demonstrated better than 3% calibration accuracy for central jets with $20\,\mathrm{GeV} < E_\mathrm{T} < 500\,\mathrm{GeV}$ [1, 2].

The primary complications of this analysis come from radiative corrections to γ+jet and the high background of QCD di-jet events where one jet is misidentified as a photon in the calorimeter. Previous studies were carried out both at particle-level [3]. These analyses focused on the modelling of detector effects, on suppressing background events and sources of a systematic shift in the jet energy scale.

This note describes the procedure for deriving the jet energy scale, with estimates of the background level and calibration uncertainties in low luminosity operation ($\mathcal{L} = 2 \times 10^{33}\,\mathrm{cm}^{-2}\mathrm{s}^{-1}$) of the LHC. The jet reconstruction algorithms used in this study are the iterative cone algorithm [4] and the cluster-based k_T-algorithm [5]. The event generation of the γ+jet signal and background processes was done with PYTHIA 6.214 [6]. The passage of particles through the detector, showering and energy loss in the calorimeters and reconstruction of the events are modelled in the CMS simulation and reconstruction packages, OSCAR 365 [7] and ORCA 871 [8], respectively.

2 Calibration procedure

The jet energy scale is set using the kinematical relationship of transverse momentum balancing between the direct photon and the jet. The measured observable

$$k_\mathrm{jet} \equiv \frac{P^\mathrm{jet}_{\mathrm{T\ meas}}}{P^\gamma_\mathrm{T}}, \tag{1}$$

provides an approximate value for the true parton-level calibration of the jet given by

$$k^\mathrm{true}_\mathrm{jet} \equiv \frac{P^\mathrm{jet}_{\mathrm{T\ meas}}}{P^\mathrm{parton}_\mathrm{T}}. \tag{2}$$

Thus, the calibration constant given by $k^\mathrm{true}_\mathrm{jet}$ is the inverse of the correction factor needed to convert the measured transverse momentum of the jet $P^\mathrm{jet}_{\mathrm{T\ meas}}$ (or its energy) to the transverse momentum of an initial parton $P^\mathrm{parton}_\mathrm{T}$ (or its energy).

The transverse momentum balance of the photon and the parton is broken by radiative corrections resulting in a two-dimensional distribution of $P^\mathrm{parton}_\mathrm{T}$ vs. P^γ_T (shown in Fig. 1a). The 2D correlation is symmetric along the line $P^\gamma_\mathrm{T} = P^\mathrm{parton}_\mathrm{T}$. Thus the $P^\gamma_\mathrm{T} - P^\mathrm{parton}_\mathrm{T}$ balance is preserved by statistically averaging over events with a fixed sum in the transverse momentum of the photon and the parton.

Calibration coefficients are determined directly in bins of P^γ_T, however, the P_T balance of the γ+parton system is broken in this case. From Fig. 1b, projecting a slice of the $P^\mathrm{parton}_\mathrm{T}$ distribution for $P^\gamma_\mathrm{T} = \mathrm{constant}$ shows a strongly asymmetric distribution with $\langle P^\mathrm{parton}_\mathrm{T} \rangle < P^\gamma_\mathrm{T}$. Even for the absolute measurement of the transverse momentum of the

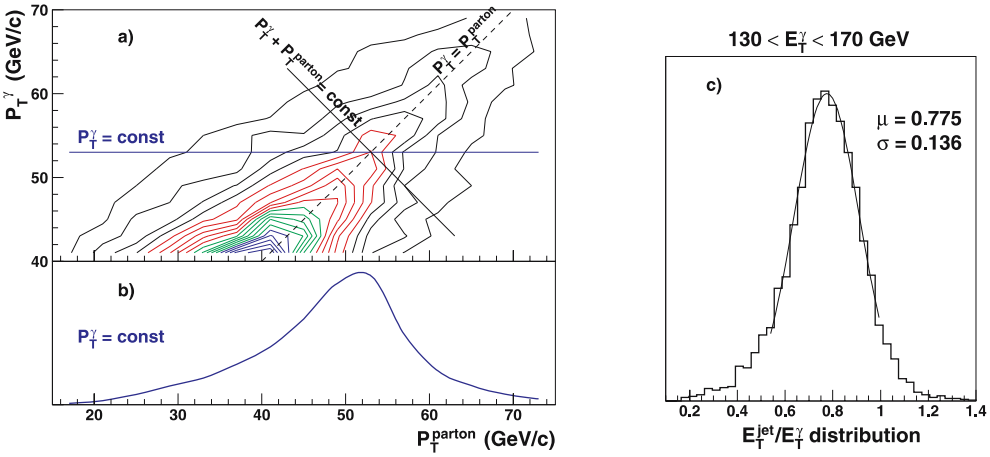

Fig. 1. a Distribution of the 2D correlation between the photon and parton transverse momenta and **b** the parton transverse momentum spectrum for a fixed photon transverse momentum in events with direct photons. **c** An example of the $E_{\mathrm{T\ meas}}^{\mathrm{jet}}/E_{\mathrm{T}}^{\gamma}$ distribution fitted with a gaussian function

parton: $P_{\mathrm{T\ meas}}^{\mathrm{jet}} = P_{\mathrm{T}}^{\mathrm{parton}}$, the value k_{jet} will contain an error from radiative corrections corresponding to:

$$\Delta = k_{\mathrm{jet}} - k_{\mathrm{jet}}^{\mathrm{true}} = \frac{P_{\mathrm{T}}^{\mathrm{parton}}}{P_{\mathrm{T}}^{\gamma}} - 1.$$

This error is significant (6.3% for $P_{\mathrm{T}}^{\gamma} = 100$ GeV). However, the position of the maximum of the $P_{\mathrm{T}}^{\mathrm{parton}}/P_{\mathrm{T}}^{\gamma}$ spectrum peaks near unity. The difference between the peak position and the P_{T}^{γ} constitutes 4% for events with $P_{\mathrm{T}}^{\gamma} = 20$ GeV and becomes as small as 0.6% at 100 GeV. Therefore, the error Δ can be reduced by defining the calibration coefficients k_{jet} to correspond to the peak of the $P_{\mathrm{T\ meas}}^{\mathrm{jet}}/P_{\mathrm{T}}^{\gamma}$ spectrum. In this study the position of the peak is determined from the mean value of a Gaussian distribution with an appropriate choice of fitting range in the vicinity of the maximum of the $P_{\mathrm{T\ meas}}^{\mathrm{jet}}/P_{\mathrm{T}}^{\gamma}$ spectrum as shown in Fig. 1c.

Table 1. The generated PYTHIA processes for γ+jet signal and background

ISUB	Subprocess
14	$f + \bar{f} \to g + \gamma$
29	$f + g \to f + \gamma$
11	$f + f' \to f + f'$ (QCD)
12	$f + \bar{f} \to f' + \bar{f}'$
13	$f + \bar{f} \to g + g$
15	$f + \bar{f} \to g + \gamma^*/Z^0$
16	$f + \bar{f}' \to g + W^{\pm}$
18	$f + \bar{f} \to \gamma + \gamma$
19	$f + \bar{f} \to \gamma + \gamma^*/Z^0$
20	$f + \bar{f}' \to \gamma + W^{\pm}$
28	$f + g \to f + g$
30	$f + g \to f + \gamma^*/Z^0$
31	$f + g \to f' + W^{\pm}$
53	$g + g \to f + \bar{f}$
68	$g + g \to g + g$

3 Events selection and systematic shifts

Events from QCD di-jet production where one jet is misidentified as photon are indistinguishable from the γ+jet calibration processes, namely, "Compton-like" $qg \to q + \gamma$ and "annihilation" $q\bar{q} \to g + \gamma$ processes.

The principal cuts to reduce the background have been shown in [3]. In these studies an efficient background suppression has been obtained using tight photon isolation cuts, a cut on azimuthal angle between the photon and the jet and a cut on the maximum transverse energy of additional jets. However, the detector effects were not included. With these effects taken into account, background suppression is less efficient. The influence of background on the calibration is investigated in this study.

Events are generated with PYTHIA 6.214 [6] specifying processes with direct photons: ISUB=14, 29 (see Table 1) for the γ+jet signal. The backgrounds were taken to be QCD and standard model processes with sufficent cross-sections to contribute to the event selection: ISUB= 11-13, 15-16, 18-20, 28, 30-31, 53, 68. In the event generation, events are required at particle-level to have a energetic isolated electromagnetic cluster:

- At least 20 GeV of transverse energy deposited in an area corresponding to the size of a 2×2 array of crystals of the electromagnetic calorimeter,
- Less than 15 GeV in the cone of radius $R = 0.5$ outside of the central array.

Events which satisfy these criteria were passed through the full detector simulation and reconstruction with the programs OSCAR 365 [7] and ORCA 871 [8]. Approximately 0.5 million events were simulated by the CMS Monte Carlo production team for use in this analysis [9].

The selection of events at the detector level was done by tightening the cuts on photon isolation, the angle between the photon and the jet ($\Delta\phi_{\gamma,jet}$) and on transverse energy of additional jets in event ($E_{\mathrm{T}}^{\mathrm{jet2}}$). The last cut is applied on raw (uncalibrated) jet energy. As a measure of the photon isolation, the value of $E_{\mathrm{T}\gamma}^{\mathrm{isol}}$ is defined to be the scalar sum of the transverse energy in the cells of the calorimeter within a cone of radius $R = 0.7$ in η-ϕ-space with repect to the direction of the parton and ouside a central array of 7×7 crystals in the electromagnetic calorimeter. The

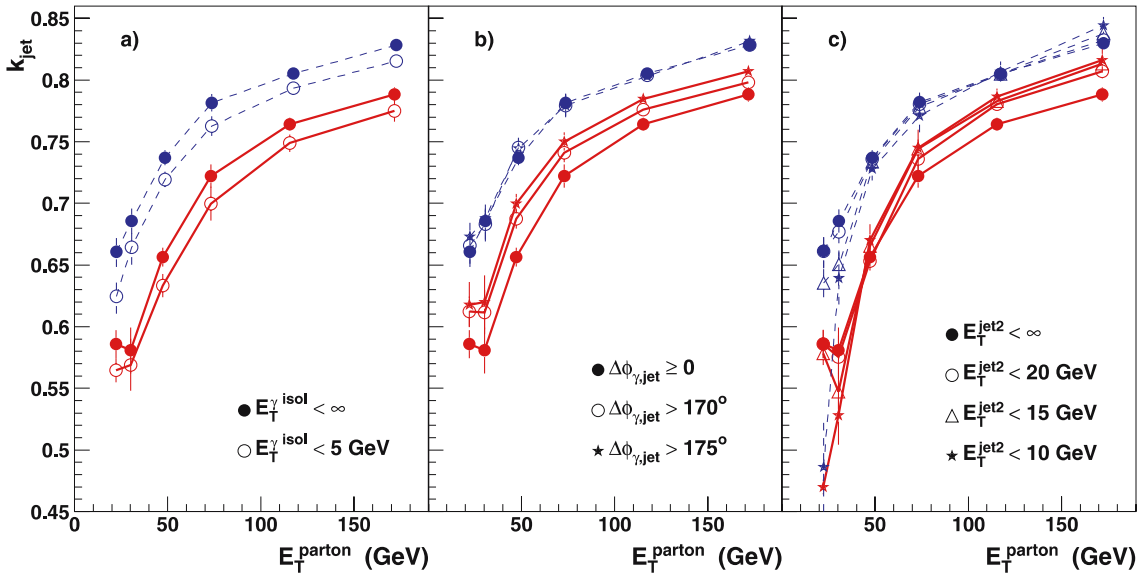

Fig. 2. True ($k_{\rm jet}^{\rm true}$, *dashed lines*) and measured (k_{jet}, *solid lines*) values of the calibration coefficients in events with direct photons for various cuts on the event selection: **a** photon isolation ($E_{\rm T\,\gamma}^{\rm isol}$), **b** the angle between the photon and the jet ($\Delta\phi_{\gamma,\rm jet}$) and **c** the transverse energy of additional jets in the event ($E_{\rm T}^{\rm jet2}$).In each case only one cut is applied (no cuts on other variables). The jets are reconstructed with the iterative cone jet algorithm with a cone radius $R = 0.5$ and calorimeter cell thresholds of $E_{\rm T}^{\rm tower} > 0.5$ GeV

sum was computed for crystals above a threshold of 0.18 and 0.9 GeV for the barrel and endcap of the electromagnetic calorimeters, respectively, and for HCAL cells above 1 GeV threshold. A cut on $E_{\rm T\,\gamma}^{\rm isol}$ defined in this way gave the largest background suppression while keeping high signal efficiency, resulting in approximately a factor of 2 loss in signal efficiency.

In Fig. 2 the effect of the cuts is shown on the true and measured values of the calibration coefficients in signal events (events with direct photons and without background from QCD di-jet events).

The cut on photon isolation has a visible influence on the calibrations, thereby affecting the systematic shift in the jet energy scale. As some level of photon isolation cut is required to suppress background, the cut is kept as loose as possible. Cutting on the angle $\Delta\phi_{\gamma,\rm jet}$ has a negligible bias on the true values of the calibration coefficients and at the same time reduces the systematic shifts in the measured calibration constants, bringing the measured values of $k_{\rm jet}$ closer to the true values. Cutting on the transverse energy of additional jets gives a similar effect at large values of the photon transverse energy, but worsens the calibra-

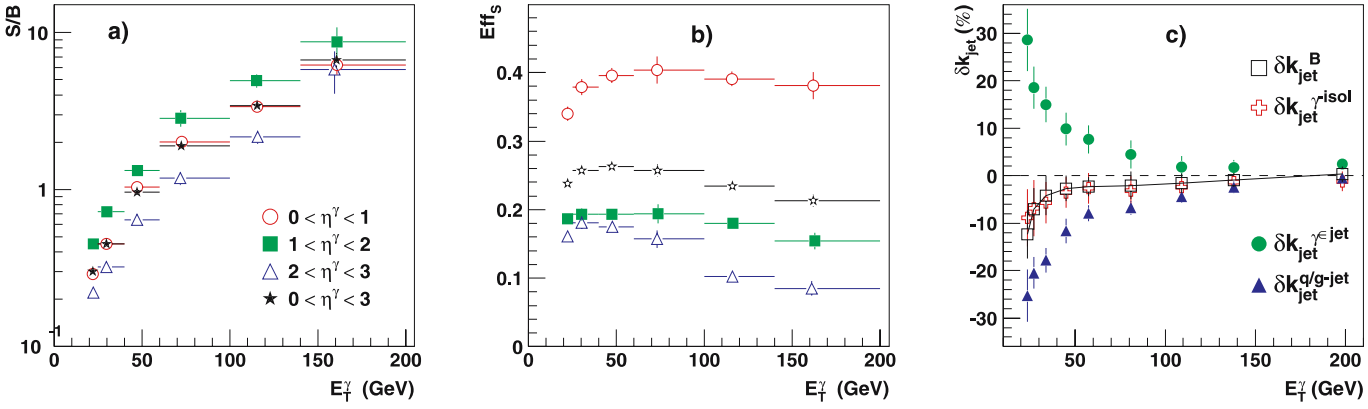

Fig. 3. **a** The ratio of signal to background after event selection and **b** the signal efficiency versus transverse energy in various regions of pseudo-rapidity of the photon with event selection cuts (3). **c** The relative systematic shift due to the presence of background events in the calibration $\delta k_{\rm jet}^{B} = \Delta k_{\rm jet}^{B}/k_{\rm jet}^{S}$ and its contributions due to the photon isolation cut ($\delta k_{\rm jet}^{\rm isol}$), the momentum imbalance from misidentified photons ($\delta k_{\rm jet}^{\gamma\in\rm jet}$) and the effect of increased gluon jet backgrounds on the average jet response ($\delta k_{\rm jet}^{q/g\text{-jet}}$) for events selected with $|\eta_{\rm jet}| < 1.5$

tion in the range of $P_{\mathrm{T}}^{\mathrm{parton}} < 40$ GeV for cut values smaller than 20 GeV.

In Fig. 3a–b, the ratio of signal to background in the selected sample and the efficiency of the signal selection are plotted as a function of photon transverse energy and for several ranges of detector pseudo-rapidity of the photon.The data are selected with the following cuts:

$$E_{\mathrm{T}\,\gamma}^{\mathrm{isol}} < 5\,\mathrm{GeV}, \quad \Delta\phi_{\gamma,\mathrm{jet}} > 172^{\circ}, \quad E_{\mathrm{T}}^{\mathrm{jet2}} < 20\,\mathrm{GeV}. \quad (3)$$

The jets are reconstructed with the iterative cone jet algorithm for a cone radius of $R = 0.5$ and with cuts on the transverse energy of the towers $E_{\mathrm{T}}^{\mathrm{tower}} > 0.5$ GeV. For this selection, the signal efficiency is about 25%. In the region of $E_{\mathrm{T}}^{\gamma} < 40$ GeV the background dominates the signal and at $E_{\mathrm{T}}^{\gamma} > 150$ GeV the background is suppressed well below the signal level.

The systematic shift due to the presence of background is given by the difference

$$\Delta k_{\mathrm{jet}}^{B} = k_{\mathrm{jet}} - k_{\mathrm{jet}}^{S},$$

where k_{jet} is the predicted value (1) calculated using all selected events passing the cuts (3) and k_{jet}^{S} is calculated from signal events after cuts are applied on the angle $\Delta\phi_{\gamma,\,\mathrm{jet}}$ and on additional jets. For signal events, the photon isolation cut which is intended to reduce background is not applied.

One contribution to this shift comes from the photon isolation cut – the difference of the calibration coefficients with ($k_{\mathrm{jet}}^{S,\,\mathrm{isol}}$) and without ($k_{\mathrm{jet}}^{S}$) a cut on photon isolation in signal events:

$$\Delta k_{\mathrm{jet}}^{\mathrm{isol}} = k_{\mathrm{jet}}^{S,\,\mathrm{isol}} - k_{\mathrm{jet}}^{S}.$$

As shown in Fig. 3c, the component $\Delta k_{\mathrm{jet}}^{\mathrm{isol}}$ approximately coincides with the total effect from background events in the calibration sample $\Delta k_{\mathrm{jet}}^{B}$. Therefore, for these values of the cuts, the calibration coefficients derived from signal and background events are expected to yield similar values. However, the calibration from background events has systematic biases not present in signal events. The background "photon" carries only part of the energy of the parton from the hard process. This breaks the P_{T} balance between the leading jet and the background "photon" and introduces a shift in the measured jet energy scale given by the difference of the calibration coefficients (1), calculated

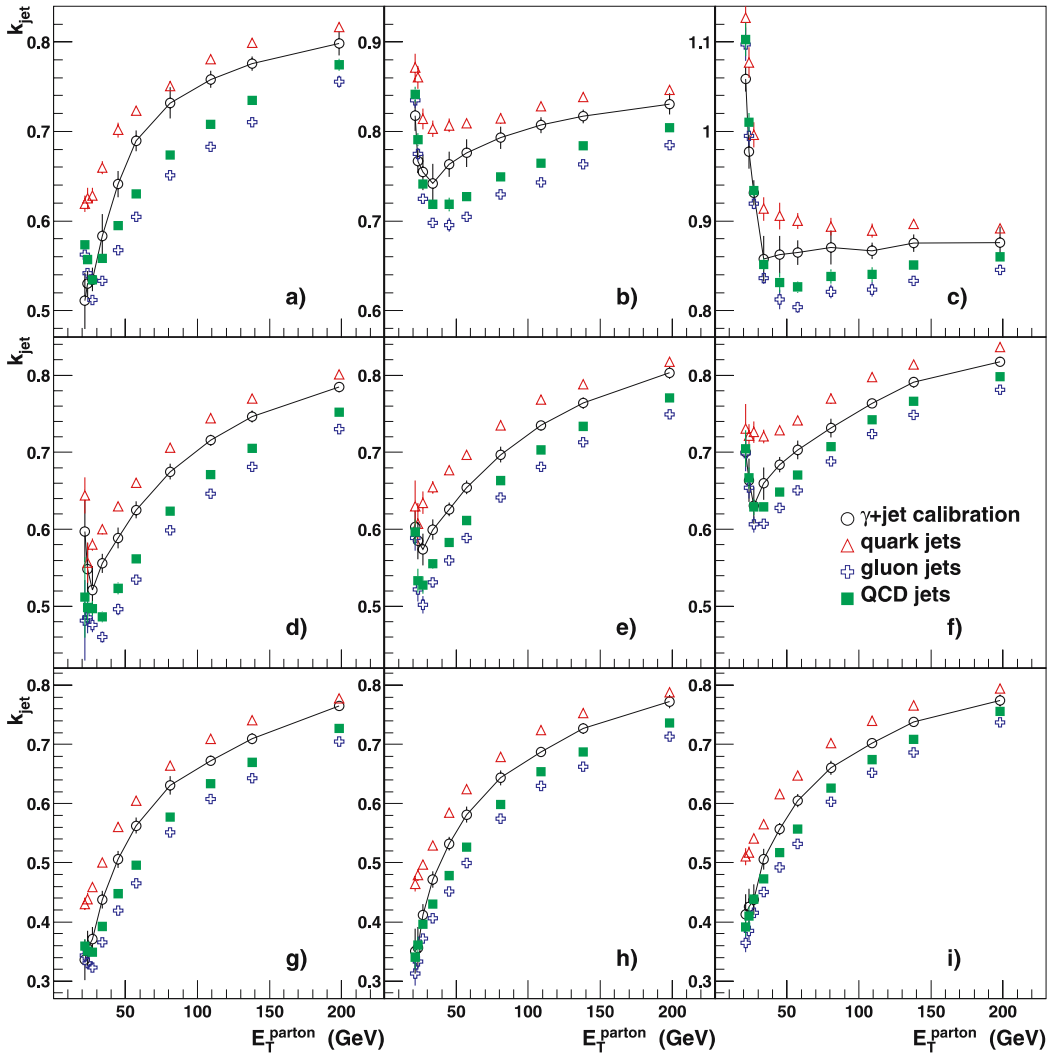

Fig. 4. The predicted values of calibration coefficients (*circles*) and their true values for quark (*triangles*), gluon (*crosses*) and any QCD jet (*squares*) for the iterative cone algorithm with cone radii of $R = 0.5$ (**a**, **d**, **g**) and $R = 0.7$ (**b**, **e**, **h**) and the k_{T}-cluster algorithm using the E_{T}-scheme (**c**, **f**, **i**) for the following thresholds on the calorimeter cells: $E_{\mathrm{T}}^{\mathrm{tower}} > 0.5$ GeV (**a**–**c**), $E^{\mathrm{tower}} > 1$ GeV (**d**–**f**) and $E^{\mathrm{tower}} > 1.5$ GeV (**g**–**i**) for $|\eta_{\mathrm{jet}}| < 1.5$

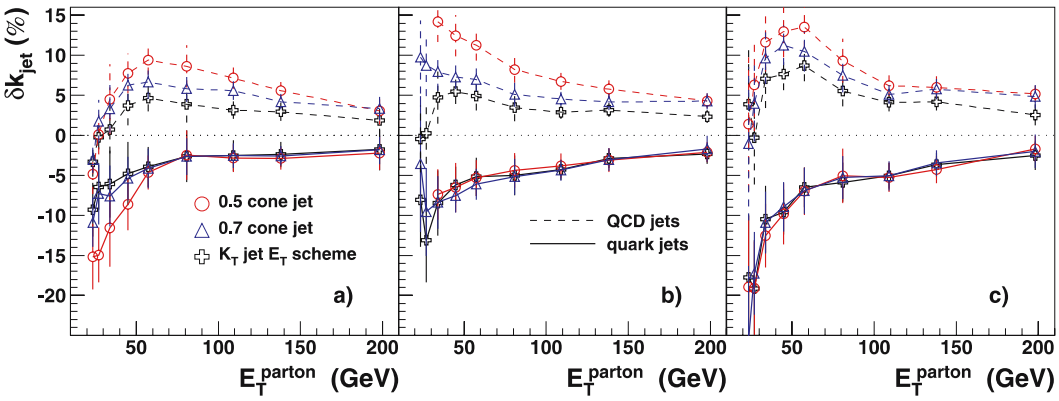

Fig. 5. Relative systematic shifts, $\frac{k_{\rm jet}-k_{\rm jet}^{\rm true}}{k_{\rm jet}^{\rm true}}$, on the calibration of quark (*solid lines*) and QCD jets (*dashed lines*) for the iterative cone algorithm with cone radii of $R=0.5$ (*circles*) and $R=0.7$ (*triangles*) and for the $k_{\rm T}$-cluster algorithm using the $E_{\rm T}$-scheme (*crosses*) for the following thresholds on calorimeter cells: **a** $E_{\rm T}^{\rm tower}>0.5$ GeV, **b** $E^{\rm tower}>1$ GeV and **c** $E^{\rm tower}>1.5$ GeV

with measured values of $P_{\rm T}^{\gamma}$ and the calibration coefficients $k_{\rm jet}^{\gamma\to{\rm parton}}$ resulting from the replacement of $P_{\rm T}^{\gamma}$ with the transverse momentum of the parton which initiated the jet misidentified as a photon:

$$\Delta k_{\rm jet}^{\gamma\in{\rm jet}}=k_{\rm jet}-k_{\rm jet}^{\gamma\to{\rm parton}}.$$

This shift reaches $10\div30\%$ at $E_{\rm T}^{\gamma}=40\div20$ GeV. However, the background response partially compensates this shift whereby unlike signal events gluon jets dominate over quark jets. The ratio of the gluon to quark jet response leads to a difference in true values of the calibration coefficients in selected events ($k_{\rm jet}^{\rm true}$) and signal events ($k_{\rm jet}^{{\rm true},S}$):

$$\Delta k_{\rm jet}^{q/g\text{-jet}}=k_{\rm jet}^{\rm true}-k_{\rm jet}^{{\rm true},S}.$$

This difference depends on the choice of jet algorithm and in cases where more energy is collected from the gluon jets, there is a partial cancellation between this systematic shift and the shift $\Delta k_{\rm jet}^{\gamma\in{\rm jet}}$. This results in an overall shift due to the presence of background in the calibration that is smaller than each of these systematics evaluated separately. The model-dependence of this cancellation as a source of additional systematic shift is not evaluated here.

In Fig. 4 the predicted values are presented for the calibration coefficients and their true values for the quark, gluon and any QCD-jet, for the iterative cone jet algorithm with cone radii of $R=0.5$ and $R=0.7$ and for the $k_{\rm T}$-clustering algorithm using the $E_{\rm T}$-scheme with various cuts on the energy and transverse energy of the cells.

Depending on the algorithm, its parameters and calorimeter cell thresholds, there is a corresponding steepness of the $E_{\rm T}$-dependence of the calibration coefficients and a spread of their values for quark and gluon jets. A strong $E_{\rm T}$-dependence and large spread in response contributes to the shift in the calibration.

The calibration shifts computed as the differences between the predicted and true values are shown in Fig. 5. The shifts for quark jets are less sensitive to the jet algorithm compared to gluon jets and contribute approximately $15\div2\%$ at $P_{\rm T}^{\rm parton}=20\div200$ GeV. Approximately the same range of systematic shifts for any QCD-jet is expected in the case of the $k_{\rm T}$-clustering algorithm. At $P_{\rm T}^{\rm parton}<50$ GeV these errors decrease due to the large collection efficiency of the jet algorithm. The calibration shifts for QCD jets depend on the algorithm and its parameters. It should be noted that the range of shifts do not characterize the quality of jet algorithm. Comparing the effect of thresholds on the calorimeter cell readings, it is found that the lowest thresholds $E_{\rm T}^{\rm tower}>0.5$ GeV and the largest effective number of calorimeter cells in the jet algorithm ($k_{\rm T}$-algorithm) yield the most uniform calibration coefficients. Greater uniformity is expected with no thresholds applied to the calorimeter cells.

4 Trigger issues and statistical uncertainties

In Fig. 6a the expected number of signal events is plotted versus photon $E_{\rm T}$ for integrated luminosity $L=10\,fb^{-1}$.

With specific triggers, a sufficient fraction of these signal events including the triggered background processes can be kept for calibration purposes.

At first trigger level the calibration data can be selected with the CMS standard single e/γ trigger. With 20 GeV threshold this selection has better than 90% efficiency for photons with $E_{\rm T}>22$ GeV [10]. The standard high-level trigger selection, however, envisages an 80 GeV $E_{\rm T}$ threshold in the single isolated photon stream to limit the final event rate to permanent storage [11]. A dedicated HLT selection is therefore needed for calibration events with lower photon energies. One possibility is to extend the standard HLT single photon selection to lower energies and prescale the output rate to an acceptable value. It should be noted, however, that the data sample in such a case would be still dominated by QCD di-jet events and a great fraction of events would be rejected by the offline selections, reducing the effective statistics available for calibration. For larger event statistics it is advantageous to move as many selections as possible (ideally all selections) to the HLT. On the

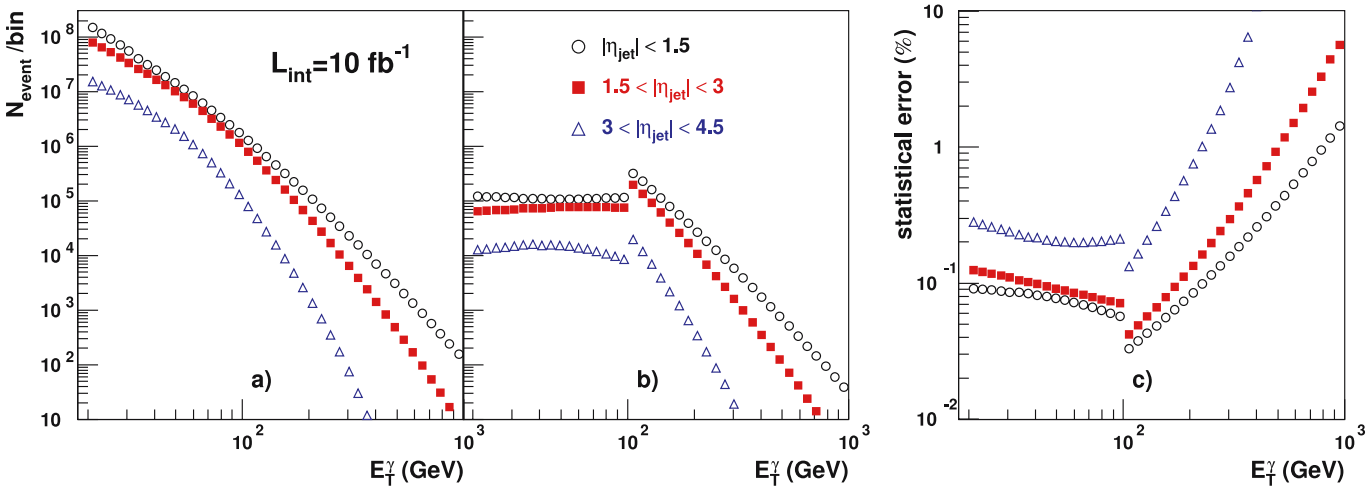

Fig. 6. a The number of events with direct photons observable in the detector acceptance for three jet pseudo-rapidity regions for integrated luminosity $L = 10\, fb^{-1}$, **b** the number of events selected for calibration for a combination of prescaled and unprescaled triggers after event selections in the HLT and offline selection efficiencies and **c** statistical errors on the jet energy scale calibration versus photon E_{T}. The bin width is 10% of the photon E_{T}. The prescaled calibration trigger below 100 GeV and the single isolated photon trigger above 100 GeV are used

other hand, the final offline selections will be the subject of systematic studies with real data, therefore looser selections should be applied in the HLT.

Our choice for the HLT selections is to use the standard isolated single photon stream with the photon Et threshold of 20 GeV and apply to the photon candidates stronger isolation cuts consistent with the offline selections. Other selections, based on an azimuthal angle cut and veto on additional jets, will be retained for offline systematic studies. The calibration event rate will be prescaled to a value consistent with the overall resources for output to storage. In Fig. 6b is shown the estimated number of calibration events versus the photon E_{T} for integrated luminosity $L = 10\, fb^{-1}$ assuming a 1 Hz trigger rate is available for calibration. We also assumed here 50% efficiency of the offline selections for events selected with the dedicated calibration trigger and 25% efficiency for events selected with the standard photon trigger. The energy dependence of the prescale factor was set so that the statistical error on the calibration was epproximately constant over the range $20\ \mathrm{GeV} < E_{\mathrm{T}}(\mathrm{jet}) < 100\ \mathrm{GeV}$.

As shown in Fig. 6c, the statistical error achieved with the prescaled trigger will be less than 1%. For jets that are calibrated with the unprescaled single photon trigger the uncertainty will be smaller at $E_{\mathrm{T}}(\mathrm{jet}) = 100\ \mathrm{GeV}$ but will grow rapidly with higher energies. The available statistics will provide statistical errors on the calibration of the order of 1% up to $E_{\mathrm{T}}^{\mathrm{jet}} \approx 1000\ \mathrm{GeV}$ (in the central region $|\eta_{\mathrm{jet}}| < 1.5$).

5 Particle-level jet energy scale

For comparison of experimental jet distributions with theoretical predictions, corrections relating reconstructed jet energies to particle-level jet energies may be needed. Such corrections can be obtained from the jet corrections to the parton level by applying an additional correction factor that relates parton energy to the particle jet energy. In the CDF experiment, it has been shown that total energy of particles in various cones in the vicinity of a parton is well simulated by PYTHIA [12]. This would enable the parton energy scale to be corrected to the particle-level jet energy scale, via Monte Carlo derived correction factors:

$$k_{\mathrm{ptcl}} \equiv \frac{P_{\mathrm{T\ ptcl}}^{\mathrm{jet}}}{P_{\mathrm{T}}^{\mathrm{parton}}}. \qquad (4)$$

QCD processes with a wide range of transverse momenta were generated using PYTHIA 6.214 (MSEL=1; ISUB=11, 12, 13, 28, 53, 68). In Fig. 7 the values of these corrections are shown for quark, gluon and any QCD-jet, collected in cones of radii $R = 0.5$ and $R = 0.7$. These co-

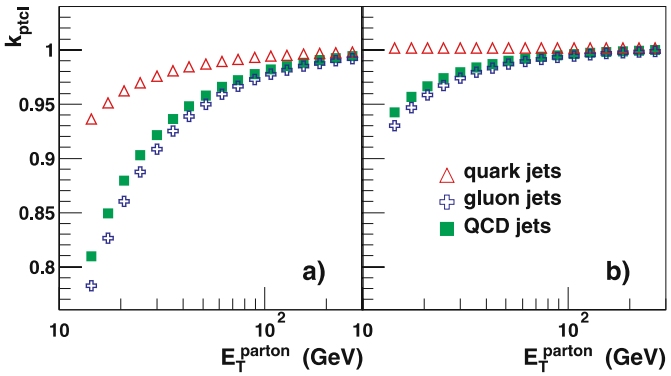

Fig. 7. Ratio of transverse momenta of particle-level jets to the transverse momenta of the initial partons for QCD, quark and gluon jets collected in cones of **a** $R = 0.5$ and **b** $R = 0.7$ at $|\eta_{\mathrm{jet}}| < 1.5$ as a function of transverse parton energy. These corrections are computed with PYTHIA 6.214

efficients (4) are characterized by a weak dependence on pseudo-rapidity (their deviations from the mean value in interval $0 < |\eta_{\rm jet}| < 4$ at fixed transverse partons energy lie within 1%) and for large transverse energies are close to unity. For quark jets and a cone radius of $R = 0.7$, the correction to parton energy is insignificant. The $E_{\rm T}$- and η-dependences of the corrections are readily derived using this technique.

6 Conclusion

Events with direct photons provide an estimate for the parton energy scale. A major challenge in the application of this technique is the imbalance imposed by radiative corrections. The effects of this problem can be greatly reduced by defining calibration coefficients in bins of photon energy and using the peak of the $E^{\rm jet}_{\rm T\,meas}/E^{\gamma}_{\rm T}$ spectrum for events passing the selection criteria.

The process γ+jet can provide sufficient statistics for the calibration of jets up to an $E^{\rm jet}_{\rm T} \approx 1000\,{\rm GeV}$.

The main background comes from QCD di-jet events where a jet is misidentified as a photon. For values of the photon transverse energy $20 \div 150\,{\rm GeV}$ the ratio of the signal to background for selected calibration events is expected to be at the level $0.3 \div 7$. Thus the background contributes to a corresponding shift in the measured jet energy scale of $12 \div 1\%$. While it is expected that a higher precision of calibration coefficients will ultimately be derived from events with a direct Z boson recoiling off a jet with much lower backgrounds, the channel $\gamma+$ jet can be used in the specified region for initial calibrations while there is still insufficient statistics in Z+jet events. In the region of $E^{\gamma}_{\rm T} > 150\,{\rm GeV}$ the $\gamma+$ jet channel is expected to have higher statistics than the Z+jet channel.

Depending on the jet algorithm, algorithm parameters and the calorimeter cell thresholds in energy and transverse energy, there is a corresponding steepness of the calibration coefficients in $E_{\rm T}$ and a spread in the response for quark and gluon jets. These dependences introduce shifts in the calibration coefficients. The shifts are estimated for quark and QCD-jets to be approximately $15 \div 2\%$ for $E^{\gamma}_{\rm T} = 20 \div 200\,{\rm GeV}$.

Using a Monte Carlo simulation of the quark and gluon fragmentation processes it is possible to estimate corrections (4) for quark, gluon and any QCD-jet to convert between a parton energy scale to a particle-level jet energy scale. The possibility of using such corrections have been studied in previous hadron collider experiments. The corrections are readily computed and have a weak dependence on pseudo-rapidity and transverse energy of the parton, especially for quark jets.

References

1. B. Abbot et al., Nucl. Instr. and Meth. A **424**, 352 (1999)
2. CMS TDR, CERN/LHCC 97-32 (1997) 387.
3. D. Bandourin, V. Konoplyanikov, N. Skachkov, Part. Nucl. Lett. **103**, 34 (2000)
4. G. Sterman, S. Weinberg, Phys. Rev. Lett. **39**, 1436 (1977)
5. S. Catani et al., Phys. Lett. B **269**, 432 (1991)
6. T. Sjostrand et al., Comp.Phys.Com. **135**, 238 (2001)
7. http://cmsdoc.cern.ch/OSCAR/
8. http://cmsdoc.cern.ch/orca
9. http://cms00.phys.ufl.edu/cms/DC04/PCP/
10. CMS TDR, CERN/LHCC 2000-038, 52 (2000)
11. CMS TDR, CERN/LHCC 2002-026, 296 (2002)
12. T. Affolder et al., FERMILAB-PUB-01/211-E